

# QUANTUM DYNAMICS OF COUPLED BOSONIC WELLS WITHIN THE BOSE-HUBBARD PICTURE

Roberto Franzosi , Vittorio Penna ,

*Dipartimento di Fisica & Unità INFN, Politecnico di Torino  
Corso Duca degli Abruzzi 24, I-10129 Torino, Italy.*

and

Riccardo Zecchina

*Condensed Matter Section, International Center of Theoretical Physics  
Strada Costiera 11, 34100 -Trieste, Italy*

## Abstract

We relate the quantum dynamics of the Bose-Hubbard model (BHM) to the semiclassical nonlinear equations that describe an array of interacting Bose condensates by implementing a standard variational procedure based on the coherent state method. We investigate the dynamics of the two-site BHM from the purely quantum viewpoint by recasting first the model within a spin picture and using then the related dynamical algebra. The latter allows us to study thoroughly the energy spectrum structure and to interpret quantally the classical symmetries of the two-site dynamics. The energy spectrum is also evaluated through various approximations relying on the coherent state approach.

## 1 Introduction

The simplest way to describe an array of interacting bosonic wells is represented by the second quantized Hamiltonian for charged bosons

$$H_{BH} = \sum_i [-\mu n_i + U n_i(n_i - 1)] - \frac{T}{2} \sum_{\langle i,j \rangle} (a_i^+ a_j + a_j^+ a_i), \quad (1)$$

where the operators  $n_i \doteq a_i^+ a_i$  count the number of bosons at the lattice site  $i$ , and the destruction (creation) operators  $a_i$ , ( $a_i^+$ ) obey the canonical commutation relations  $[a_i, a_j^+] = \delta_{ij}$ . The parameters  $T$ ,  $U > 0$ , and  $\mu$  represent the hopping amplitude, the strength of the Coulomb on-site repulsion, and the chemical potential, respectively.

Hamiltonian (1), known in the literature [1] as the Bose-Hubbard Model (BHM), was originally derived as the lattice version of the second quantized  $|\Psi|^4$ -field theory used to model superfluids adsorbed in porous media. It describes in fact a gas of identical charges that hop through a  $D$  dimensional lattice, and exhibit a repulsive action whenever two (or more) charges are situated at the same site. The bosonic character of the lattice stands in the fact that, in principle, an unlimited number of charges is allowed to occupy each lattice sites. On this account the BHM is able to mimic appropriately various features of systems such as granular superconductors, short-length superconductors and Josephson junction arrays, hence deserving a growing attention in the recent years (see references in Ref. [2]). For the same reason the BHM seems to supply the appropriate theoretic framework in which describing an array of interacting Bose-Einstein condensates.

The recent years have been characterized by remarkable progresses in constructing experimental devices able to confine some hundreds of bosons so as to form real Bose-Einstein condensates (BEC) [3]. This has prompted as well the investigation of more structured situations in which two condensates (regarded as sites or wells filled by condensed bosons within the BHM picture) can interact via tunneling processes [4]. In particular, a quite rich scenery of dynamical behaviors has been found to characterize the two-site case (named boson Josephson junction) in Ref. [5], where two coupled Gross-Pitaevskii equations for two condensate wavefunctions are assumed as the minimal interaction scheme whereby describing interwell processes. This represents however the most general array of coupled BEC's so far realized even if BEC's with complex architectures have been constructed [6], and a large amount of both experimental and theoretic work has been devoted to construct arrays within the physics of uncondensed ultracold atoms in optical lattices (see Refs. [7], [8] and references therein).

Despite its almost purely theoretic value, it is interesting to illustrate for conceptual reasons the link between the BHM and a system of many bosonic wells regarded as interacting Bose condensates. We reconstruct such a correspondence in Sec. 2 for the general case and employ it in Sec. 3 to show how the two-site BHM coincides, in a semiclassical picture, with a two-condensate system.

In this paper we shall focus our attention on the quantum dynamics of the two-site case. Classically, the problem is known to be integrable since the dynamics of the complex site variables  $z_1, z_2$  required to account for the system state (these identify with the wavefunctions of the two-condensate system) can be recast in terms of two action-angle variables by exploiting the constant of motion  $\mathcal{N} \equiv |z_1|^2 + |z_2|^2$ . The reliability of the classical picture comes, of course, from the fact that indeed the operators  $n_\ell$  counts a large number of particle and thus identifies with its semiclassical counterpart  $|z_\ell|^2$  via the correspondence scheme discussed in Sec. 2.

A smaller number of particles per site makes reasonable recovering the quantum picture both because this is experimentally possible, and because it is interesting to investigate thoroughly the changes in the structure of the quantum states when going from the pure quantum regime to situations with an intermediate, more or less pronounced, semiclassical character. Moreover, it is important to recall that the BHM exhibits a zero temperature  $\mu$ - $T$  phase diagram which contains regions of finite size (lobes) where the system loses its superfluid character becoming an insulator [1, 2]. In this respect we are interested in making evident the cause of the presence of insulator regions in the phase diagram in relation with the structure of the two-site model eigenstates.

In Sec. 3 we review the semiclassical form of the two-site dynamics and implement the standard requantization procedure for comparing it to the spectrum provided by the exact quantum treatment. In order to study the quantum dynamics of the two-site BHM in Sec. 4 we represent the Hamiltonian within a spin algebra realization based on the generators of  $\text{su}(2)$ , in which the index of the algebra representation is proportional to the total boson number  $N$ . This establishes the equivalence between the usual description of the BHM Hilbert space through the bosonic Fock basis and a simplified picture relying on the angular momentum eigenstates. The latter, in turn, allows one to use the  $\text{su}(2)$  coherent states (where the conservation of the total boson number has been already incorporated) when performing the classical limit.

The spin picture also provides the basis for developing in Sec. 5 the single-boson picture of the system dynamics. This amounts to reconstructing the exact dynamical algebra [9] of the two-site BHM. Explicitly, the model is reformulated within an enlarged algebra –which identifies with  $\text{su}(N+1)$  in its fundamental representation– where the two-site Hamiltonian takes the form of a many-boson Hamiltonian on a  $(N+1)$ -site lattice whose population is formed by a unique (effective) boson. The algebraic formulation we introduce is viable to BHM’s with more than two site and provides a deeper insight of the dynamics complexity from the group-theoretic standpoint. Moreover, it appears particularly advantageous in studying the quantum counterpart of the nonintegrable classic dynamics of the  $N$ -site BHM ( $N > 2$ ). This problem will be considered elsewhere.

At the operational level, such an approach entails a reformulation of the quantum dynamics in terms of a (classical) Hamiltonian which exhibits a quadratic dependence on the components of the  $\text{su}(2)$  picture states. In particular, such an Hamiltonian is employed in Sec. 6 to analyse various dynamical regimes and to recognize the distinctive characters of both the superfluid and the insulator behavior.

## 2 Arrays of condensates within the BHM picture

The link that relates the BHM to a system of interacting boson condensates is easily established by implementing the method used in Refs. [2, 10] for investigating the quantum dynamics of many-particle lattice models. To this end the one-dimensional (1D) Hamiltonian derived from (1)

$$H_c = \sum_{j=1}^M \left[ -\mu n_j + U n_j (n_j - 1) - \frac{T}{2} \left( a_j^\dagger a_{j+1} + a_{j+1}^\dagger a_j \right) \right], \quad (2)$$

suffices to generate a chain of  $M$  interacting wells namely the generalization of the case with two interacting condensates.

The method just mentioned combines the generalized coherent state picture of quantum systems with the time-dependent variational principle (TDVP) [9], and allows one to reformulate the quantum dynamical problem relative to (2) by a semiclassical hamiltonian dynamics in terms of the expectation values

$$z_j := \langle Z | a_j | Z \rangle, \quad z_j^* := \langle Z | a_j^\dagger | Z \rangle \quad (3)$$

and generated within the TDVP procedure by Hamiltonian  $\mathcal{H}_c(Z, Z^*) \doteq \langle Z | H_c | Z \rangle$ . The so-called trial macroscopic wave function  $|Z\rangle$  here is assumed to have the form  $|Z\rangle = \prod_j |z_j\rangle$ , where  $1 \leq j \leq M$  and  $|z_j\rangle$  are the Glauber coherent states [9] solutions of the standard equation  $a_j |z_j\rangle = z_j |z_j\rangle$  for each  $j$ . The dynamical equations for  $z_j$  (those for  $z_j^*$  are obviously obtained by complex conjugation)

$$i\hbar \dot{z}_j = (2U|z_j|^2 - \mu)z_j - \frac{T}{2} \sum_{i \in (J)} z_j \quad (4)$$

are derived [2] from the semiclassical Hamiltonian

$$\mathcal{H}_c(Z, Z^*) \equiv \sum_j \left[ (-\mu + U|z_j|^2)|z_j|^2 - \frac{T}{2} \left( z_j^* z_{j+1} + z_{j+1}^* z_j \right) \right], \quad (5)$$

through the standard formulas  $\dot{z}_j = \{z_j, \mathcal{H}_c\}$  based on the canonical Poisson brackets  $\{z_j^*, z_\ell\} = (i/\hbar)\delta_{j,\ell}$ . It is easily checked as well that the basic feature  $[H_c, N] = 0$  of the quantum system has a classical counterpart given by  $\{\mathcal{H}_c, \mathcal{N}\} = 0$ , where  $\mathcal{N} \equiv \sum_\ell |z_\ell|^2$ . The identification of  $z_j$  with the wavefunction of the  $j$ -th condensate establishes the link claimed above, showing explicitly that the effective dynamics of BHM generates the classical dynamics of coupled condensates.

### 3 Semiclassical picture of the two-well system

It is interesting to derive the two-well dynamics from the general case of the  $M$ -site lattice described by Hamiltonian (5). Upon assuming  $z_{2s} = z_2$  and  $z_{2s+1} = z_1$  (suppose that  $M$  is even and the lattice is endowed with periodic boundary condition), (5) leads to the two-site Hamiltonian

$$\mathcal{H} := \mathcal{H}_c/(M/2) \equiv \left[ U(|z_1|^4 + |z_2|^4) - \mu(|z_1|^2 + |z_2|^2) - T(z_1^* z_2 + z_2^* z_1) \right], \quad (6)$$

while (4) reduce to the two equations

$$\begin{cases} i\hbar\dot{z}_1 = (2U|z_1|^2 - \mu)z_1 - Tz_2 \\ i\hbar\dot{z}_2 = (2U|z_2|^2 - \mu)z_2 - Tz_1 \end{cases}. \quad (7)$$

This amounts to considering a special solution characterized by two independent complex variables with  $|z_1|^2 + |z_2|^2$  representing the constant of motion. Remarkably, the same equations are obtained independently when assuming  $\mathcal{H}$  to be the two-site Hamiltonian equipped with the Poisson brackets  $\{z_a, z_b^*\} = \delta_{ab}/i\hbar$ ,  $a, b = 1, 2$ . It is easily recognized that  $q$ -site models, where  $qp = M$  for some  $p \in \mathbf{N}$ , can be achieved by following the same procedure ( $z_{\alpha+kq} \equiv \xi_\alpha$ ,  $0 \leq k \leq p$ ,  $1 \leq \alpha \leq q$ ) and that their dynamics can always interpreted as solutions of the  $M$ -site model exhibiting the discrete translation symmetry  $z_{j+kq} = z_j$ ,  $\forall j$ ,  $0 \leq k \leq p$ . The physical interpretation of such a symmetry is given by the Fourier modes description of the dynamical variables  $\sqrt{M}b_q = \sum_j z_j \exp[i\tilde{q}j]$ , where  $\tilde{q} := 2\pi q/M$ ,  $j, q \in [1, M]$ , and  $M\delta(j-\ell) \equiv \sum_q \exp[i\tilde{q}(j-\ell)]$ . By inserting the condition  $z_2 = z_{2s}$  and  $z_1 = z_{2s+1}$  one finds  $b_0 \equiv \sqrt{M}(z_1 + z_2)/2$ , and  $b_{M/2} \equiv \sqrt{M}(z_1 - z_2)/2$  that imply

$$z_1 = (b_0 + b_{M/2})/(2\sqrt{M}), \quad z_2 = (b_0 - b_{M/2})/(2\sqrt{M}).$$

Therefore the two-site model represents the simplest possible way to construct an excited state with respect to the condensed macroscopic state characterizing the zero temperature regime where  $z_j = b_0/\sqrt{M}$ ,  $\forall j$ . Hamiltonian (6) can be rewritten as

$$\mathcal{H} \equiv \left[ \frac{U}{2}\mathcal{N}^2 - \mu\mathcal{N} + \frac{U}{2}D^2 - T\sqrt{\mathcal{N}^2 - D^2}\cos(2\theta) \right], \quad (8)$$

where we have introduced the new canonical variables  $\mathcal{N} = |z_1|^2 + |z_2|^2$ ,  $D = |z_1|^2 - |z_2|^2$ ,  $\theta = (\phi_1 - \phi_2)/2$ , and  $\psi = (\phi_1 + \phi_2)/2$  implied by  $z_j = |z_j|\exp(i\phi_j)$ . The new coordinates are equipped with the Poisson brackets

$$\{\theta, \mathcal{N}\} = 0 = \{\psi, D\}, \quad \{\theta, D\} = -1/\hbar = \{\psi, \mathcal{N}\},$$

that provide the equation of motions

$$\dot{D} = 2T\sqrt{\mathcal{N}^2 - D^2} \sin(2\theta), \quad \dot{\theta} = -UD - \frac{TD}{\sqrt{\mathcal{N}^2 - D^2}} \cos(2\theta), \quad (9)$$

the dot denotes the time derivative  $d/d\tau$  with  $\tau := t/\hbar$ . Based on the complete integrability of the system, and proceeding along the same lines of Ref. [10], one can reduce the above two equations to a unique one

$$\dot{D}^2 = -4 \left( E - U\mathcal{N}^2/2 + \mu\mathcal{N} - UD^2/2 \right)^2 + 4T^2(\mathcal{N}^2 - D^2), \quad (10)$$

where  $E = \mathcal{H}$  is a given value of the energy, which reproduces the result achieved in Ref. [11]. Going to its second order version

$$\ddot{D} = (a - bD^2) D,$$

where  $a = 4U\epsilon - 4T^2$ ,  $b = 2U^2$ , and  $\epsilon = E - U\mathcal{N}^2/2 + \mu\mathcal{N}$  (reduced energy), allows one to represent its solution in terms [12] of the elliptic cosine  $cn(x; k)$ . This has the form  $D(t) = \mathcal{A} cn[\lambda(\tau - \tau_0); k]$ , in which  $\mathcal{A}^2 = (1 + a/\lambda^2)/(b\lambda^2)$ ,  $k = (1 + a/\lambda^2)/2$ , and  $\lambda$  is a scale time that can be fixed arbitrarily [12].

In order to implement the requantization procedure a la Brillouin-Einstein-Keller [13] the complete set of the fixed point is requested. These are

$$\theta = 0, \quad D = 0, \quad (\text{minimum}) \quad (11)$$

$$\theta = \pm\pi/2, \quad D = \pm\sqrt{\mathcal{N}^2 - (T/U)^2}, \quad (\text{maxima}) \quad (12)$$

$$\theta = \pm\pi/2, \quad D = 0, \quad (\text{saddle points if } T/U < \mathcal{N}) \quad (13)$$

with (reduced) energy  $\epsilon$

$$\epsilon_m = -T\mathcal{N}, \quad \epsilon_M = \frac{U}{2}(\mathcal{N}^2 + T^2/U^2), \quad \epsilon_S = +T\mathcal{N}, \quad (14)$$

respectively. The structure of the  $D - \theta$  phase space depends on the parameter  $\Gamma := T/\mathcal{N}U$ . For  $\Gamma < 1/2$  the domains containing the maxima (consider, for example, those related to  $\theta = \pi/2$  represented in Fig. 1a) are confined by a separatrix

$$D_M^{(\nu)}(\theta) = \nu\mathcal{N}\sqrt{1 - 4\Gamma^2 \cos^2(2\theta)}, \quad (15)$$

with  $\nu = +1$  ( $\nu = -1$ ) for the upper (lower) maxima, that corresponds to the energy  $\epsilon_* = U\mathcal{N}^2/2$ . Such disjoint domains are separated by a region for whose orbits  $\theta$  can increase indefinitely. Another pair of separatrices confine the curves encircling

the minimum. These are obtained from (8) by setting the reduced energy  $\epsilon$  equal to  $\epsilon_S$  and read

$$D_m^\pm(\theta) = \pm\sqrt{2}\mathcal{N} \left[ 1 - \Gamma \cos^2(2\theta) \pm \cos(2\theta)\sqrt{\Gamma^2 \cos^2(2\theta) + (1 - 2\Gamma)} \right]^{1/2}. \quad (16)$$

For  $\Gamma = 1/2$  the separatrices of the two maxima intersect in  $\theta = \pi/2$ ,  $D_m^\pm = 0$  thus eliminating the possibility of ballistic evolution of the phase. At the same time (see Fig. 1b) they merge with the minimum separatrices (16).

For  $\Gamma > 1/2$  two-branch separatrix (15) forms a unique curve which is displaced vertically and join the upper boundary of the phase space ( $D_M = \mathcal{N}$ ) to the lower one ( $D_M = -\mathcal{N}$ ). The values in the interval  $1/2 < \Gamma < 1$  correspond to situations in which a new eight-shaped separatrix encircles the two maxima (see Fig. 2a) and divides the curves of motion that locally surround each maxima from those that contain both. Equation (16) still describes such a separatrix centered in the saddle point ( $D_m^\pm = 0$ ,  $\theta = \pi/2$ ), but it is convenient to introduce the variable  $\phi := \theta - \pi/2$  in view of the fact that  $(1 - 2\Gamma)$  is now negative. In the limit  $\Gamma \rightarrow (1/2)^+$  the vertical separatrix and the eight-shaped separatrix merge, while for  $\Gamma \rightarrow 1^-$  the maxima merge (see Fig. 2b) thus generating a configuration with a unique maximum which characterizes  $\Gamma \geq 1$ .

An approximate evaluation of the energy level distribution can be easily obtained for curves of motion close to the extremal points just introduced. Upon expressing  $D$  as a function of  $\theta$

$$D^\pm(\theta) = \nu\mathcal{N}\frac{\sqrt{2}}{U} \left[ \frac{2\epsilon}{U\mathcal{N}^2} - \Gamma^2 c^2(\theta) \pm \Gamma c(\theta)\sqrt{\Gamma^2 c^2(\theta) + 1 - \frac{2\epsilon}{U\mathcal{N}^2}} \right]^{\frac{1}{2}}, \quad (17)$$

with  $\nu = \pm 1$  and  $c(\theta) = \cos(2\theta)$ , the requantization procedure is enacted by setting

$$\oint_\gamma D d\theta \equiv 2\pi(n + 1/2), \quad (18)$$

where  $n \in \mathbf{N}$ ,  $\gamma$  is some isoenergetic closed path, and the constant  $\hbar$  is missing since  $D$  is a dimensionless action variable.

In general, the exact calculation of the above integral is quite difficult. Therefore it is convenient to reduce  $H$  to a diagonal quadratic form in proximity of both minima and maxima. In the case of the minimum ( $D/\mathcal{N} \ll 1$ ,  $\theta \ll 1$ ) the resulting Hamiltonians reads

$$\mathcal{H}_m \simeq \frac{U\mathcal{N}^2}{2} - \mathcal{N}(T + \mu) + \frac{U}{2}(1 + \Gamma)D^2 + 2T\mathcal{N}\theta^2, \quad (19)$$

while the maxima entail a quadratic Hamiltonian

$$\mathcal{H}_M \simeq U\mathcal{N}^2 - \mu\mathcal{N} + \frac{T^2}{2U} + \frac{U}{2}[1 - \Gamma^{-2}]p^2 - 2(T^2/U)\phi^2, \quad (20)$$

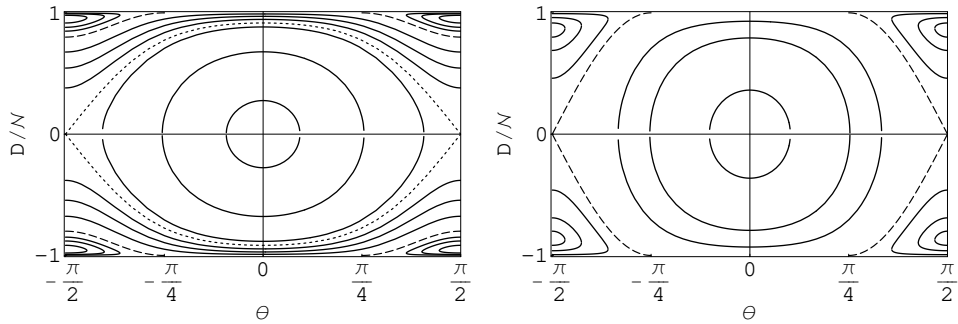


Figure 1: (a) left figure illustrates the minimum separatrix (dotted lines) and the two separatrices (dashed lines) associated to each maximum pair for  $\Gamma < 1/2$ ; (b) right figure shows the merging of separatrices for  $\Gamma = 1/2$ .

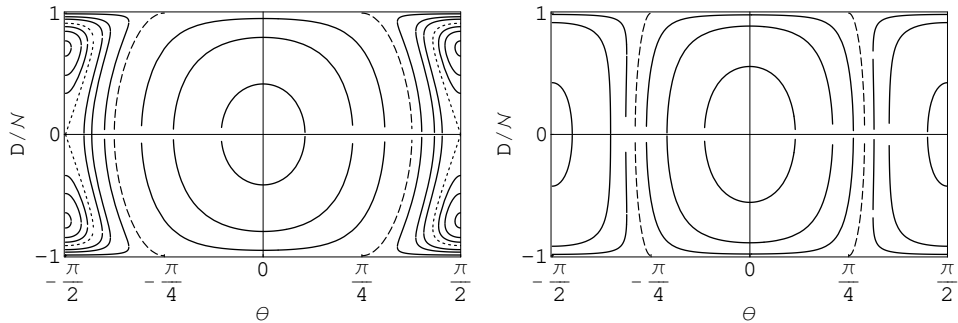


Figure 2: (a) left figure illustrates the eight-shaped separatrix encircling each maximum pair for  $1/2 < \Gamma < 1$ ; (b) right figure shows the phase space for  $\Gamma > 1$ .



with  $p := [(D/\mathcal{N}) \pm (1 - \Gamma^2)^{1/2}] \ll 1$ ,  $\phi \simeq \theta \pm \pi/2$ . Under such approximations the integral (18) can be easily calculated and provides the approximate form of the spectra

$$E_m(n) = U\mathcal{N}^2 \left[ \frac{1}{2} - \frac{\mu}{U\mathcal{N}} - \Gamma + \sqrt{\Gamma(1 + \Gamma)} (2n + 1) \right] \quad (21)$$

and

$$E_M(n) = U\mathcal{N}^2 \left[ 1 - \frac{\mu}{U\mathcal{N}} + \frac{\Gamma^2}{2} - \sqrt{1 - \Gamma^2} (2n + 1) \right]. \quad (22)$$

for the minimum and the maxima, respectively.

The case when the Hamiltonian exhibits two maxima is quite interesting in that the presence of pairs of isoenergetic trajectories (spatially disjoint) suggests the possibility for the system to undergo a tunneling effect when considered quantum-mechanically. Indeed this is the case for  $\epsilon_S < \epsilon < \epsilon_M$ , and  $1/2 < \Gamma < 1$  where isoenergetic trajectories appear around the points

$$P_R := (+\mathcal{N}\sqrt{1 - \Gamma^2}, \pm\pi/2), \quad P_L := (-\mathcal{N}\sqrt{1 - \Gamma^2}, \pm\pi/2),$$

in the phase plane  $(D, \theta)$ . Due to the tunneling effect, close to the value  $\Gamma = 1/2$  the first order corrections in  $\hbar$  must be accounted when approximating the energy levels.

A simple way to evaluate such an effect is obtained via the following standard scheme [14] showing how the tunneling probability is nonvanishing when the barrier that separates the motions around  $P_R$  and  $P_L$  is finite. In this case a new relevant contribution (to the second order in the perturbative approximation) must be added to the energy levels (22).

Let  $H_R$  and  $H_L$  be the quadratic approximation of  $H$  around  $P_R$  and  $P_L$ , respectively, and  $|\Psi_R\rangle$  and  $|\Psi_L\rangle$  the eigenstates of  $H_R$  and  $H_L$  corresponding to the same eigenvalue  $E_M(n)$ ; the two eigenvalues:

$$E_{\pm}(n) = E_M(n) \mp \hbar^2 \left[ \Psi_R \frac{d\Psi_R}{dD} \right]_C, \quad (23)$$

where  $C$  is the crossing point  $(D, \theta) = (0, \pi/2)$ , correspond then to the symmetric/antisymmetric states:  $|\Psi_{\pm}\rangle = (|\Psi_R\rangle \pm |\Psi_L\rangle)/\sqrt{2}$ . At the second order we have

$$\left[ \Psi_R \frac{d\Psi_R}{dD} \right]_C = \frac{\omega}{2\pi\hbar} \exp \left[ -\frac{1}{\hbar} \int_{-a}^a dD |p(D)| \right], \quad (24)$$

where  $\omega \equiv (U\sqrt{\Gamma^{-2} - 1})/(2T)$ ,  $p(D) \equiv [2\omega(\hbar n/2 - 2\omega D^2/U)]^{1/2}$ , and the inversion points  $D = \pm a$  of the motion along  $D$  have been issued from (17) by setting  $\theta = \pi/2$  in  $D^+(\theta)$ .

## 4 The spin picture of the quantum dimer

The Hamiltonian of a lattice formed by two sites (dimer) reads

$$H = U(n_1^2 + n_2^2) - (\mu + U)N - T(a_1a_2^+ + a_2a_1^+), \quad (25)$$

where now  $N \equiv n_1 + n_2$ , whereas the factor  $T$  of the hopping term in place of  $T/2$  is the only difference distinguishing the open chain case from the case with the periodic boundary conditions  $a_{M+j} = a_j$  with  $M = 2$ . Upon introducing the two-boson realization of the  $\text{su}(2)$  generators

$$J_1 = \frac{1}{2}(a_1a_2^+ + a_2a_1^+), \quad J_2 = \frac{1}{2i}(a_1a_2^+ - a_2a_1^+), \quad J_3 = \frac{1}{2}(n_2 - n_1) \quad (26)$$

which satisfy the commutators

$$[J_1, J_2] = iJ_3, \quad [J_2, J_3] = iJ_1, \quad [J_3, J_1] = iJ_2,$$

and the Casimir equation  $C \doteq J_1^2 + J_2^2 + J_3^2 \equiv J_4(J_4 + 1)$  with  $J_4 = \frac{1}{2}(n_2 + n_1)$ , Hamiltonian (25) can be rewritten in the nonlinear form

$$H = 2[UJ_4^2 - (\mu + U)J_4 + UJ_3^2 - TJ_1]. \quad (27)$$

This fact has two consequences: First, the size of the Hilbert space of the system, encoded in the eigenvalue  $J$  of  $J_4$ , is related explicitly to a macroscopic feature of the system since  $2J_4$  coincides with the total particle number operator  $N$ . The latter naturally plays the role of constant of motion within our group-theoretic picture in that  $J_4$  is a group central element that is  $[J_4, J_a] = 0$ ,  $a = 1, 2, 3$ . Moreover, (27) shows how, due the nonlinear term  $J_3^2$ ,  $H$  cannot be diagonalized via a simple unitary transformation of the group  $\text{SU}(2)$ . In view of the nonlinearity of (27) the problem of diagonalizing  $H$  for any value of  $J$  can be faced either by expressing  $J_3^2$  (and  $J_1$ ) linearly in terms of the generators of a larger (dynamical) algebra, or by constructing approximation procedures capable of retaining the relevant features of the spectrum. The latter point of view is assumed in this Section.

Consider first the low part of the spectrum of  $H$ , the features of which should be relevant to the zero temperature phase diagram of the BH model. The spin formulation of the problem allows one to implement an approximate approach based on the Casimir operator. In fact, the observation that the classical energy minimum is reached for  $J_3 = J_2 = 0$ , and  $J_1 = +\sqrt{C}$ , where  $C = J_1^2 + J_3^2 + J_2^2$  is a constant, leads to approximate  $J_1$  as  $J_1 \simeq \sqrt{C}[1 - (1/2C)(J_3^2 + J_2^2)]$  which implies

$$H \simeq 2 \left\{ UJ_4^2 - (\mu + U)J_4 + UJ_3^2 - T\sqrt{C} \left[ 1 - \frac{1}{2C}(J_3^2 + J_2^2) \right] \right\}. \quad (28)$$

The variables  $J_3, J_2$  (considered "small") account for small displacements around the energy minimum. At the quantum level, the inequalities  $\langle J_s \rangle \ll \sqrt{C}$  concerning the expectation values of  $J_s$ , with  $C = J(J+1) = N(N+2)/4 \gg 1$ , and  $s = 2, 3$  make natural to adopt the perturbative scheme where the operator  $J_2$  and  $J_3$  can be treated as canonically conjugate variables since

$$[J_2, J_3] \simeq +i\sqrt{C}, \quad (29)$$

whereas

$$[J_3, J_1] = +i\sqrt{C}(J_2/\sqrt{C}) \simeq 0, \quad [J_2, J_1] = -i\sqrt{C}(J_3/\sqrt{C}) \simeq 0, \quad (30)$$

are considered vanishing when compared with (29) since  $\langle J_s \rangle/\sqrt{C} \ll 1$ . Then, after labelling by the integer  $p$  the eigenstates of the harmonic oscillator term  $[1 + T/(2U\sqrt{C})][J_3^2 + W^2 J_2^2]$  contained in (28), where  $W^2 = [1 + 2U\sqrt{C}/T]^{-1}$ , its eigenvalues are found to be  $\sqrt{C}W(2p+1)$  so that the spectrum of  $H$  reads

$$E_p = \frac{U}{2}N^2 - (\mu + U)N - 2T\sqrt{C} + T \left[ 1 + \sqrt{C} \frac{2U}{T} \right]^{\frac{1}{2}} (2p+1). \quad (31)$$

The approximation just implemented is of course exact for  $UN = 0$ . Hence its natural range of validity seems to be given by the condition  $T/NU \geq 1$ , which can be interpreted semiclassically as the requirement that the expectation value of the hopping term  $T|\langle J_1 \rangle| \simeq TN/2$  is greater than the (maximum value of the) Coulomb expectation value  $U\langle J_3^2 \rangle \simeq UN^2/4$ . This appears to be consistent with the fact that the harmonic oscillator form of the above spectrum is originated by the spectrum of  $J_1$  which is both linear and bounded from below. When  $T/NU < 1$  the spin structure of the problem fully emerges since  $J_3^2$  introduce the influence of its quadratic degenerate spectrum.

The importance of the condition  $T/NU \geq 1$  is even more evident when describing the spectrum close to the maximum energy configuration. In this case the approximation  $J_1 \simeq -\sqrt{C}[1 - (1/2C)(J_3^2 + J_2^2)]$  makes appear in  $H$  the harmonic oscillator term  $-[T/(2U\sqrt{C}) - 1][J_3^2 + \Omega^2 J_2^2]$  where  $\Omega^2 = T/(T - 2U\sqrt{C})$  which involves a spectrum of the form

$$E_q = \frac{U}{2}N^2 - (\mu + U)N + 2T\sqrt{C} - T \left[ 1 - \sqrt{C} \frac{2U}{T} \right]^{\frac{1}{2}} (2q+1). \quad (32)$$

For  $T/NU < 1$  the system no longer exhibits a unique maximum so that the oscillator approximation of the problem does not work: the squared frequency  $\Omega^2$  becomes imaginary. The spin picture thus appears as the correct approach for understanding quantum mechanically the degeneracy caused by the presence of two (classical) symmetric maxima for  $T/NU < 1$ .

## 5 Two-well system dynamical algebra

### 5.1 Single-boson picture

Considering the subalgebra  $\text{su}_N(2)$ , in the spin representation  $J = N/2$  where  $N$  is the total number of boson, within the algebra  $\mathcal{A} = \text{su}(M)$  allows us to recast the nonlinear Hamiltonian  $H$  in terms of a linear combination of generators belonging to  $\mathcal{A}$ . The latter is therefore a *dynamical algebra* for the system. The simplest possible choice for  $\mathcal{A}$  is provided by the two-boson operator realization of  $\text{su}_Q(M)$  the generators of which have the standard form

$$E_{ij} := b_i^+ b_j, \quad (i \neq j), \quad H_{ij} := (b_i^+ b_i - b_j^+ b_j)/2 \quad (33)$$

with  $1 \leq i, j \leq M$ , and satisfy the commutation relations

$$[E_{ij}, H_{kl}] = \frac{1}{2} (\delta_{jk} E_{ik} - \delta_{jl} E_{il} + \delta_{il} E_{lj} - \delta_{ik} E_{kj}) \quad , \quad [E_{ij}, E_{kl}] = \delta_{jk} E_{il} - \delta_{il} E_{kj} .$$

The index  $Q$  eigenvalue of the invariant operator  $N_b = \sum_i b_i^+ b_i$  ( $[N_b, E_{ij}] = 0$ ) that selects the specific representation of  $\text{su}(M)$  considered, denotes the total number of particle associated with such a bosonic realization of  $\text{su}(M)$ . In fact, the dimension of the Hilbert space basis  $B(M, Q) = \{|n_1, \dots, n_M\rangle, \sum_{i=1}^M n_i = Q\}$  is given by  $\dim B(M, Q) = (Q + M - 1)! / [(M - 1)! Q!]$ , where the basis states are defined as  $|n_1, \dots, n_M\rangle = \otimes_{i=1}^M |n_i\rangle$  and the number operator states  $|n_j\rangle$  fulfil the equations  $b_i |n_i\rangle = \sqrt{n_i} |n_i - 1\rangle$  and  $b_i^+ |n_i\rangle = \sqrt{n_i + 1} |n_i + 1\rangle$ .

Setting  $M=N+1$  (recall that  $N$  is the boson number of the two-well system) and  $Q=1$  one selects the fundamental realization of  $\text{su}(M)$ , whose one-boson quantum states  $|0, \dots, 1, 0, \dots\rangle$  ( $\dim B(N+1, 1) \equiv N+1$ ) are in one-to-one correspondence with the column vector standard basis whose matrix form reads  $\{|1\rangle := (1, 0, \dots)^T, |2\rangle := (0, 1, \dots)^T, \dots, |q\rangle := (0, \dots, 1, 0, \dots)^T\}$ . The generators of the resulting matrix realization of  $\text{su}_1(N+1)$  have the form

$$\|E_{ij}\|_{qp} \equiv \delta_{qi} \delta_{jp} \quad , \quad \|H_{ij}\|_{qp} \equiv \frac{1}{2} (\delta_{qi} \delta_{ip} - \delta_{qj} \delta_{jp}) \quad ,$$

where  $1 \leq q, p \leq M = N + 1$ . The states  $|J; m\rangle$  constituting the standard basis of  $\text{su}_N(2)$  can be similarly realized within the column vector basis  $\{|q\rangle, 1 \leq q \leq N+1\}$  via the identification  $|J; m\rangle \equiv |q\rangle$  with  $m = J + 1 - q$ . The ensuing matrix version of the  $\text{su}_N(2)$  generators reads

$$\|J_+\|_{qp} \equiv \sqrt{(p-1)(2J+2-p)} \delta_{q, p-1} \quad , \quad \|J_3\|_{qp} \equiv (J-p+1) \delta_{qp}$$

thus entailing that  $J_+$  and  $J_3$  can be rewritten within  $\mathfrak{su}(M)$  (recall that  $M \equiv N+1$ ) as

$$J_+ = \sum_{q=1}^{N+1} \sqrt{q(2J+1-q)} E_{q, q+1}, \quad J_3 = \sum_{q=1}^{N+1} \frac{J+1-q}{M} \left[ Q - 2 \sum_{j=1}^M H_{jq} \right], \quad (34)$$

respectively. Formally, this turns out to be equivalent to representing our quantum description in the fully bosonic form, with

$$J_+ = \sum_{q=1}^{N+1} \sqrt{q(2J+1-q)} b_q^+ b_{q+1}, \quad J_3 = \sum_{q=1}^{N+1} (J+1-q) n_q,$$

with the constraint  $\sum_{q=1}^{N+1} b_q^+ b_q \equiv 1$ . Hamiltonian (27) then becomes

$$H = C(J) + 2U \sum_{q=1}^{N+1} m^2(q) n_q - T \sum_{q=1}^{N+1} R(q, J) (b_q^+ b_{q+1} + b_{q+1}^+ b_q), \quad (35)$$

where  $R(q, J) := [(J+1/2)^2 - (m(q) - 1/2)^2]^{1/2}$ ,  $m(q) := J+1-q$ , and  $C(J) = 2[UJ^2 - (\mu + U)J]$ . The related dynamics is now described by states

$$|\Psi\rangle = \sum_{q=1}^{N+1} \xi_q b_q^+ |0, \dots, 0\rangle, \quad (36)$$

that, due to the normalization condition, turn out to define the manifold  $\sum_{q=1}^{N+1} |\xi_q|^2$  in the bosonic Hilbert space. Such a manifold is an hypersphere in  $\mathbf{C}^{N+1}$  and represents the effective space in which the quantum dynamics of  $H$  can be reformulated in a classical form in such a way to maintain a complete equivalence with the original quantum problem. In fact the classical dynamics thus obtained actually concerns the time evolution of the components of  $|\Psi\rangle$  once the initial condition  $|\Psi(0)\rangle$  at  $t=0$  has been assigned.

Based on Eq. (36), the Schrödinger problem  $(i\partial_t - H)|\Psi\rangle = 0$  can be rewritten as a set of equations of motion

$$i\dot{\Psi}_m = 2Um^2 \Psi_m - T [\rho_J(m+1) \Psi_{m+1} + \rho_J(m) \Psi_{m-1}], \quad (37)$$

where we have adopted the notation  $\Psi_m := \xi_q$ , and  $\rho_J(m) := R(q, J)$  with  $m := J+1-q$ , in order to make the present formalism closer to the spin picture introduced previously. Equations (37) can be derived in an independent way from the effective Hamiltonian

$$\mathcal{H}[\Psi] = C(J) + \sum_{m=-N/2}^{N/2} \left[ 2Um^2 |\Psi_m|^2 - T \rho_J(m) (\Psi_m^* \Psi_{m-1} + \Psi_{m-1}^* \Psi_m) \right], \quad (38)$$

representing the energy expectation value  $\langle \Psi | H | \Psi \rangle \equiv \mathcal{H}[\Psi]$ , provided the Poisson structure  $\{\Psi_q, \Psi_p^*\} = \delta_{qp}/i\hbar$  is assumed. The eigenfrequencies associated to (38) and the related periodic orbits coincide with the eigenvalues and the eigenstates of (37), respectively. The latter are obtained from the solution of the secular equation

$$EX_m = 2Um^2 X_m - T [\rho_J(m+1) X_{m+1} + \rho_J(m) X_{m-1}] , \quad (39)$$

that is easily derived from the equations of motion (37). The eigenstates components  $X_m$  in Eqs. (39) can be shown to be real.

## 5.2 Spectrum structure

Two symmetries characterize the structure of the eigenstates. The first is realized via the action of the unitary transformation  $U_1 := \exp[i\pi J_1]$  which takes  $J_3$  into  $U_1 J_3 U_1^+ = -J_3$  so that  $[H, U_1] = 0$ . The action of  $U_1$  on the standard basis is given by  $U_1 |m\rangle = \exp[i\pi J] | -m \rangle$ . This corresponds to implementing the component transformation  $X_m \rightarrow sX_{-m}$  with  $s = \pm 1$  in Eqs. (39) that remain unchanged in that  $\rho_J(m+1) \equiv \rho_J(-m)$  for each  $m$ . Each eigenstate has therefore a definite symmetry character which we make explicit by writing the eigenstates as

$$|E\rangle_+ = \sum_m S_m(E) |m\rangle , \quad S_m := +S_{-m} , \quad (40)$$

$$|E\rangle_- = \sum_m A_m(E) |m\rangle , \quad A_m := -A_{-m} , \quad (41)$$

in the symmetric and antisymmetric case, respectively. The energy spectrum is not degenerate in that one has that  $E \neq E'$  for any pair of states  $|E\rangle_+$  and  $|E'\rangle_-$ .

A further symmetry is obtained by combining the action  $U_3 J_1 U_3^+ = -J_1$  of  $U_3 := \exp[i\pi J_3]$  on  $-TJ_1$  in  $H$ , with the change  $T \rightarrow -T$  which restores the initial form of  $H$ . The corresponding change of the eigenstate components  $X_m \rightarrow \exp[i\pi m] X_m$  is easily derived from the fact that the standard basis is acted on by  $U_3$  according to the formula  $U_3 |m\rangle = \exp[i\pi m] |m\rangle$ . This does not make change Eqs. (39) provided the sign of  $T$  is reversed as well.

An important feature of the eigenvalues structure is recognized by comparing the secular equations for  $|E\rangle_+$  and  $|E\rangle_-$ . We first consider the case when  $J$  is a half of an odd integer. Then equations (39) can be written in the reduced form

$$0 = (2Um^2 - E) C_m - T [\rho_J(m+1) C_{m+1} + \rho_J(m) C_{m-1}] , \quad (42)$$

with  $C = A, S$ , for  $1/2 < m \leq J$ , while for  $m = 1/2$  one has

$$0 = [2U (1/2)^2 - E] C_{1/2} - T [\rho_J(3/2) C_{3/2} + \eta \rho_J(1/2) C_{-1/2}] , \quad (43)$$

where  $\eta = -1(+1)$  must be taken in the antisymmetric (symmetric) case. The remarkable consequence of the presence of  $\eta$  in (43) is that one may distinguish the eigenvalues associated with the symmetric states from those related to the antisymmetric ones depending on the sign of  $\eta$ . How this happens is clearly shown by the eigenvalues equation. The latter is obtained iteratively via the recurrence equation for the determinant of the associated secular equation

$$d[E, m] = (2Um^2 - E) d[E, m + 1] - T^2 \rho_J^2(m) d[E, m + 2], \quad (44)$$

which terminates with  $d[E, J] = 2U J^2 - E$ , starting from

$$0 = (U/2 - E + \eta T \rho_J(1/2)) d[E, 3/2] - T^2 \rho_J^2(1/2) d[E, 5/2]. \quad (45)$$

Developing (45) by means of (44) a  $(J + 1/2)$ -th degree equation for  $E$  is obtained. For  $\eta = 0$  no difference distinguishes the symmetric case from the antisymmetric case that therefore exhibit pairs of eigenstates with the same eigenvalues. As soon as  $\eta$  is switched on each eigenvalues bifurcates relatively to the two possibilities  $\eta > 0$  and  $\eta < 0$ . For small values of  $T$  the leading order in (45) is  $T$ , so that it reduces to

$$0 = (U/2 - E + \eta T \rho_J(1/2)) \otimes_{m>1/2}^J (2Um^2 - E).$$

There results that only the two lowest eigenvalues are distinguished from those of the unperturbed case. Increasing  $T$  allows one to improve the resolution: for example, to the order  $T^2$ , the four lowest eigenvalues are separated.

The same scheme holds when  $J$  is integer ( $m = 0, 1, 2, \dots$ ) but the hierarchy described above exhibits two special cases, for  $m = 0, 1$ :

$$0 = -E C_0 - T \sigma \rho_J(1) C_1, \quad (46)$$

$$0 = (2U - E) C_1 - T [\rho_J(2) C_2 + \sigma \rho_J(0) C_0], \quad (47)$$

with  $C = A, S$ , whereas Eqs. (42) account for  $2 \leq m \leq J$ . The parameter  $\sigma$  must be set equal to one in the symmetric case ( $C = S$ ), while in the antisymmetric case ( $C = A$ ) the expected elimination of the component  $A_0$  is realized by setting  $\sigma = 0$ . It follows that the Hilbert space dimension decreases while the secular equation will have a degree diminished of one. Explicitly, one has

$$0 = -E d[E, 1] - \sigma^2 \rho_J^2(1) T^2 d[E, 2], \quad (48)$$

which reduces to  $0 = d[E, 1]$  for  $\sigma \rightarrow 0$ . In the symmetric case a  $(J + 1)$ -th degree equation for  $E$  issues from (48) through the same formula (44).

For  $T$  sufficiently small the energy levels appear to be structured in doublets (see Fig. 3) that mimick the emergence of the energy degeneracy actually reached only

for  $T = 0$ . The eigenvalues of the doublet sector satisfy the inequality  $E > TN$ , consistently with the role played classically by the saddle point energy  $\epsilon_s$  of formula (14). Thus the doublet number decreases when  $T$  is increased (see Figs. 4, 5). This effects issues from the fact that both  $\eta$  and  $\sigma$  are multiplied by  $T$  in (45) and (48), respectively. The limit  $T \rightarrow 0$  thus incorporates the limits  $\eta, \sigma \rightarrow 0$  whereby the degeneracy crops up (each  $E$  is associated to a pair  $|E\rangle_{\pm}$ ). The eigenstates generated (in the same limit)  $|E\rangle_{\pm} \equiv (|m\rangle \pm |-m\rangle)/\sqrt{2}$  have the same self-energy  $E(0) = C(J) + 2Um^2$  of the noninteracting model (competition among the  $m$  modes switched off by  $T = 0$ , that is, no interwell dynamics).

The splitting of energy levels caused by  $T \neq 0$  guarantees the important feature that eigenstates are structured so as to have components that are either symmetric or anti-symmetric with respect to the inversion  $m \rightarrow -m$ . A full degeneracy, in fact, should allow for the occurrence of states inducing a strong localization in proximity of those values of  $\langle J_3 \rangle$  that classically correspond to the energy peak positions. In this case the eigenstates should exhibit a marked semiclassical character that corresponds to states where either the components with  $m > 0$  or those with  $m < 0$  are strongly depressed in order to permit the localization effect.

Despite the absence of states involving a stable localization around one of the two energy peaks for energy values  $E > T/U$  when  $T/UN < 1$ , the realization of localized states can be attained by superpositions of the two states corresponding to the doublets. Each such a pair of states is composed by a symmetric eigenstate and an antisymmetric one with an energy gap  $\Delta E$  which vanishes for  $T \rightarrow 0$ . The configurations where the system is localized undergo a periodic revival (with a life time proportional to  $1/\Delta E$ ) which ensues from the time dependence of the eigenstate interference mechanism.

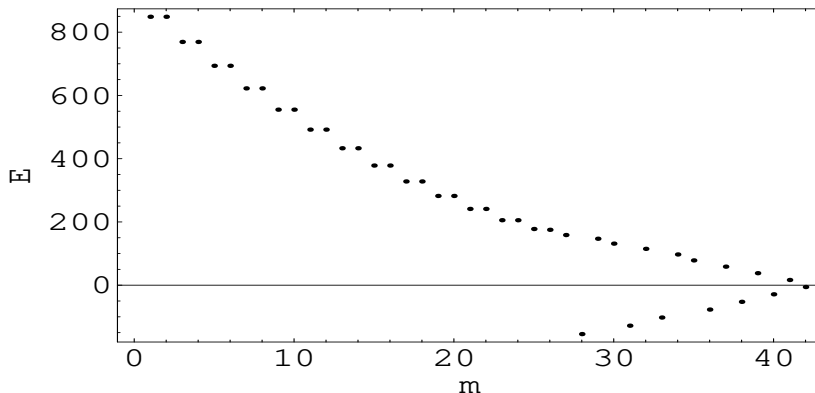


Figure 3: Energy level distribution for  $T = 4$ ,  $U = 1$ ,  $N = 41$ . The index  $m \in [1, 42]$  labels the energy eigenvalues.



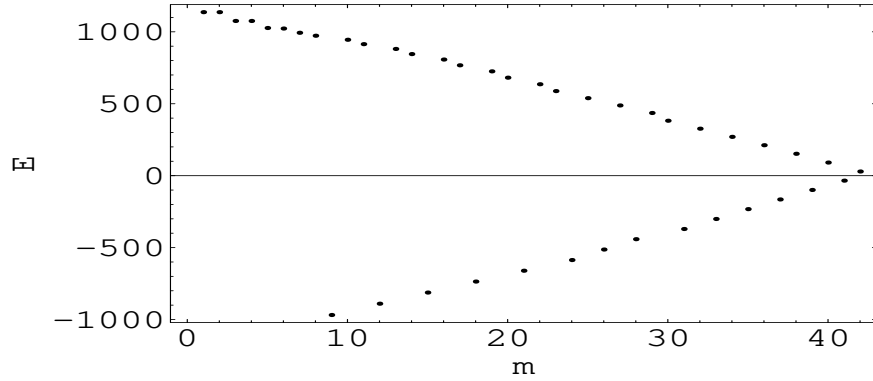


Figure 4: Energy level distribution for  $T = 24$ ,  $U = 1$ ,  $N = 41$ . The eigenvalues are labelled by the index  $m \in [1, 42]$ . Three doublets are still visible for  $m < 6$

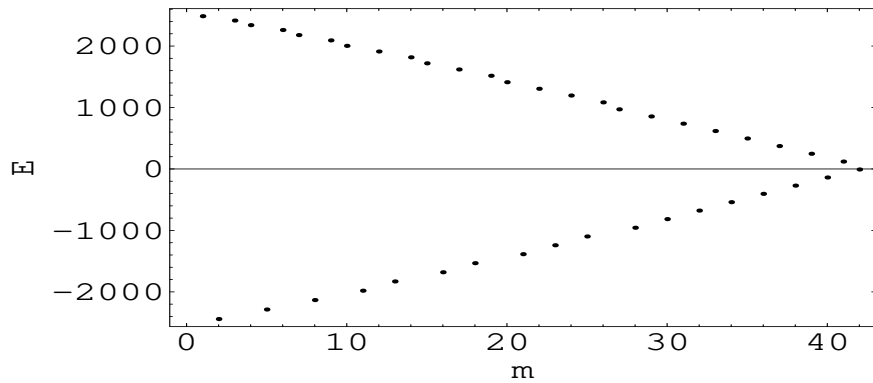


Figure 5:  $T = 60$ ,  $U = 1$ ,  $N = 41$ : the influence of  $UJ_3^2$  in Hamiltonian (27) is almost negligible.

## 6 Discussion

The structure of Hamiltonian (38) allows us to interpret the time evolution of a generic state  $|\Psi\rangle$  as the dynamics of an ensemble of linear oscillators with a space-dependent coupling ( $\rho_J(m)$  depends on  $m$ ) in the linear lattice of  $m$  modes. A certain amount of information can be extracted from (38) as to the form of the states  $|\Psi\rangle$  close to the extremal configurations.

Let us consider, first, the case  $\Gamma \simeq 1$  (we identify the classical parameter  $\mathcal{N}$  with the eigenvalue  $N = 2J$  so that  $\Gamma \equiv T/UN$ ). The greatest coefficients of the hopping term ( $\max[T\rho_J(m)] \simeq UN^2/2$ ) are comparable with the greatest coefficient of the Coulomb term ( $\max[2Um^2] = UN^2/2$ ). On the other hand, such two classes of terms involve different components that are labelled by  $m \simeq 0$  and  $m \simeq \pm N/2$ , respectively. The minimum energy state is therefore characterized by components  $\Psi_m = R_m \exp(i\alpha_m)$  such that  $\alpha_m \equiv \alpha_{m+1}$  (the phase-locking involves the most negative the hopping term), whereas the modes  $|m| \ll N/2$  ( $|m| \simeq N/2$ ) must be maximally occupied (strongly depleted). The dynamics of weakly excited states is expected to exhibit a similar mode participation with the breaking of the (collective order of the) phase-locking due to small phases' oscillations.

For opposite reasons the maximum energy state is characterized by an antiferromagnetic type of phase order ( $\alpha_{m+1} = \alpha_m + \pi$ ), while both the largest modes ( $|m| \simeq N/2$ ) and the smallest ones ( $|m| \ll N/2$ ) contribute to maximize the energy. Such a phase order enables us to recognize the largest components of the maximum energy state starting from Hamiltonian (38). Upon setting  $\alpha_m \simeq \pi + \alpha_{m-1}$  to maximize the energy, and assuming that  $\|\Psi_m| - |\Psi_{m-1}|\| \ll |\Psi_m|, |\Psi_{m-1}|$  which entails  $\Psi_m^* \Psi_{m-1} + \Psi_m \Psi_{m-1}^* \simeq -[|\Psi_m|^2 + |\Psi_{m-1}|^2]$ , Hamiltonian (38) reduces to the diagonal form

$$\mathcal{H}[\Psi] \simeq C(J) + \sum_{m=-N/2}^{N/2} \left[ 2Um^2 + T(\rho_J(m) + \rho_J(m+1)) \right] |\Psi_m|^2.$$

For large values of  $J = N/2$  the label  $m$  can be regarded as a continuous parameter so that the highest weight coefficient  $[2Um^2 + T(\rho_J(m) + \rho_J(m+1))]$  is singled out by differentiation. This provides  $m [m \pm (N^2 - T^2/U^2)^{1/2}/2] \simeq 0$  where  $m = \pm(N^2 - T^2/U^2)^{1/2}/2$  are the values for which  $|\Psi_m|$  must be maximized in order to reach to the highest energy configuration. This result matches exactly the classical representation of the maxima in the phase space (see formula (12)), except that quantum mechanically both the maxima are involved in the dynamics. If  $\Gamma \geq 1$ , the solution  $m = 0$  must be considered which reflects in a consistent way the coalescence of the two (classical) maxima in a unique one.

The regime  $\Gamma \ll 1$  is also interesting. This case is quite sensitive to the parity of  $N$  since the largest Coulomb term has gained a factor  $N$  with respect to the

largest  $T$ -dependent term. If  $N$  is even (i.e.  $m$  assumes integer values) the system ground-state must be constructed in such a way that  $|\Psi_0| \gg |\Psi_m|$  since  $|\Psi_0|$  does not contribute to the Coulomb term. We thus approximate  $|\Psi\rangle$  by neglecting any  $\Psi_m$  such that  $m \neq 0, \pm 1$ . The resulting approximation of  $\mathcal{H}[\Psi]$  reads

$$\mathcal{H}[\Psi] \simeq C(J) + 4U|\Psi_1|^2 - 4T\rho_J(0)|\Psi_1||\Psi_0|,$$

where we have assumed  $|\Psi_{+1}| \equiv |\Psi_{-1}|$ , and the constraint  $2|\Psi_{+1}|^2 + |\Psi_0|^2 = 1$  holds. The latter suggests to set  $\sqrt{2}|\Psi_{+1}| = \sin\alpha$  and  $|\Psi_0| = \cos\alpha$  in the above formula, which in turn appears to be minimized by  $\text{tg}\alpha = \sqrt{2}T\rho_J(0)/U \simeq TN/\sqrt{2}U$ . The ground-state energy thus reads

$$E_{gs} = C(J) + \frac{U}{4}[1 - \sqrt{1 + \text{tg}^2\alpha}],$$

that reproduces the semiclassical value  $E \simeq C(J) - TN$  for  $T/U \leq 1/N$ . If  $N$  is odd ( $m = \pm 1/2, \pm 3/2, \dots$ ) the Coulomb term never vanishes, and the main contributions to ground-state come from  $\Psi_{-1/2}$  and  $\Psi_{+1/2}$ , so that the related energy is approximated by

$$\mathcal{H}[\Psi] \simeq C(J) + \frac{U}{2}(|\Psi_{-1/2}|^2 + |\Psi_{+1/2}|^2) - 2T\rho_J(-1/2)|\Psi_{-1/2}||\Psi_{+1/2}|.$$

In view of the normalization  $|\Psi_{-1/2}|^2 + |\Psi_{+1/2}|^2 = 1$ , it reduces to

$$E_{gs} \simeq C(J) + \frac{U}{2} - \frac{TN}{2}\sqrt{1 + 2/N},$$

under the assumption  $|\Psi_{-1/2}| = |\Psi_{+1/2}|$ .

The characters distinguishing the even case and the odd case suggest the interpretation of such situations in terms of insulator and superfluid states, respectively. In the odd case one has  $m = \pm 1/2, \pm 3/2, \dots$  so that the ground-state is the superposition of the states  $|N/2, N/2 + 1\rangle$  and  $|N/2 + 1, N/2\rangle$  which involves a permanent one-boson tunneling between the two wells (superfluid regime). In the even case the ground-state essentially coincides with  $|J, 0\rangle \equiv |N/2, N/2\rangle$  which entails a stationary regime where the two bosonic wells are equally filled and the boson tunnelling is not favoured (insulator regime). It is worth noting that any contribution of the hopping term turns out to be definitely smaller than the Coulomb terms namely  $\max[T\rho_J(m)] \simeq U/2 < \min[U m^2] \simeq U$  when one sets  $\Gamma \equiv 1/N^2$ . The ensuing almost null importance of the hopping term is precisely the signal of the transition from the superfluid to the insulator regime which is known (see [1], [2]), for a given  $N$ , to take place at  $\Gamma \equiv 1/N^2$ .

A simple evaluation of the components  $X_m$  of the eigenstates associated with the energy spectrum extremes (where relative sign of  $X_m, X_{m+1}$  is definite) is obtained

by regarding  $m$  as a continuous parameter in Equation (39). In fact, upon setting  $X_m = Y_m/\sqrt{(J+m)!(J-m)!}$  and replacing  $Y_{m\pm 1}$  with  $Y_m \pm dY_m/dm$  in (39), one finds

$$0 = (E - 2Um^2 + 2JT)Y_m - 2T\sigma m \frac{dY_m}{dm}, \quad (49)$$

where  $\sigma = +1$  ( $-1$ ) for the minimum (maximum) energy state. The solution have the form  $Y_m = Cm^\Lambda \exp(-Um^2/2T)$  with  $\Lambda = E/(2T\sigma) - J$  and the constant  $C$  is fixed by imposing the state normalization. The same treatment can be extended to the intermediate eigenstates but the sign oscillation of  $X_m$ 's, known from numerical calculation of eigenstate, requires a more accurate reformulation of Eqs. (39) also involving a second derivative term.

## 7 Conclusions

In this paper we have focused our attention on the quantum aspects of the dynamics of a two-site Bose-Hubbard model. The latter mimicks the interaction of two BEC's via tunneling effect. This has led us to study thoroughly the nontrivial structure of the energy spectrum the upper part of which consists of a series of doublets if  $\Gamma < 1$ , and has suggested the quantal interpretation of the degeneracy characterizing the classical configurations (a pair of symmetric orbits is associated to the same value of the energy).

The general framework in which we relate the quantum dynamics of BEC's to the classical formulation usually employed for macroscopic condensates has been described in Sec. 2, where the purely quantum model of many lattice sites (bosonic wells coupled within the BHM picture) is reduced to a classical lattice field theory by means of the TDVP procedure and the coherent state representation of the macroscopic (quantum) state of the lattice gas. Conversely, such a construction shows that a generic array of coupled BEC is naturally reconducted to the standard BHM and its generalization to nonperiodic lattice structures [15] when considered in a nonclassical regime (small or mesoscopic number of bosons per condensate).

Sec. 3 has been devoted to illustrate the classical form of the two-site model, its phase space, and the orbit structure therein. After discussing the integrable character of the system the dynamics of which is completely accounted by canonical variables  $\theta, D$  (see equations (9)), the requantization procedure *a la* BEK has been implemented. This provides integral (18) whose approximate solutions give the evaluation of energy levels (21) and (22) in proximity of the minimum and the maxima, respectively. The nice feature that (22) holds for  $\Gamma < 1$  has allowed us to incorporate the exchange effects via the procedure leading to formula (23). Such a result anticipates the basic trait of the spectrum represented by its doublet structure.

The reformulation of the two-site model in terms of a macroscopic spin has been performed in Sec. 4. Such a picture offers the possibility to approximate the energy spectrum in an independent way for levels close to the minimum and maximum values. The approximation well fits the exact energy values for  $\Gamma > 1$  and shows implicitly how the exhaustive investigation of the spectrum unavoidably requires the spin picture. This paves the way for the construction of the dynamical algebra which is the base for the exact diagonalization of the model.

The realization of  $su_N(2)$  within the larger algebra  $su_Q(N+1)$  in terms of a single-boson representation ( $Q=1$ ) has been developed in Sec. 5 and supplies the spin operators in the form (34). It provides the algebraic framework where the nonlinearity of  $J_3^2$  is eliminated and the Hamiltonian becomes a linear superposition (see (35)) of  $su_1(N+1)$  generators. The procedure is easily generalized to many-site lattice [16]. The set-up developed leads to reformulate the two-site model as a  $(N+1)$ -lattice model described by the quadratic Hamiltonian (35) and a population constituted by a single particle. The spin nonlinear dynamics has been finally reconducted to a classical problem with the quadratic Hamiltonian (38) depending on the canonical variables  $\Psi_j$  (these are the components of the wavefunction solving the Schrödinger equation) and  $\Psi_j^*$ . The proper modes of (38) coincides with the eigenvalues  $E$  of  $H$  that are grouped in two sectors  $E > TN$  and  $E < TN$  if  $0 < \Gamma < 1$ . The first sector contains the doublets.

The basic result illustrated in Sec. 5 is that the levels of each doublet are associated to a symmetric state and an antisymmetric state exhibiting almost coincident secular equations. Their difference, that turns out to be concentrated in one (or two) of the equations forming the hierarchy of equations for the eigenstate components (see Eqs. (43) and (46)-(47)), has been represented via a parameter which joins analytically the symmetric and antisymmetric eigenvalues. This explains the origin of the doublet structure through a bifurcation mechanism which represents the main result of the present paper. In Sec. 6 the two site model ground-state has been interpreted for  $\Gamma \ll 1/2$  as a state with a superfluid (insulator) behavior for an odd (even) total particle number  $N$  thus showing how the germ of the lobe-like structure of the zero temperature phase diagram is already present in a two-site lattice. The method and the analysis developed in the present work can be extended to lattices with a number of sites greater than two. The bifurcation mechanism explained above is expected to provide the base for studying the chaotic character of the trimer case. Work on the three-site case is in progress along these lines [16].

## Acknowledgements

The work of R. F. has been supported by an I.N.F.M. grant. V. P. expresses his gratitude to the Condensed Matter Section of I.C.T.P. for its hospitality as well as to the M.U.R.S.T. for financial support within Project SINTESI.

## References

- [1] M.P.A. Fisher, B. P. Weichman, G. Grinstein, and D. S. Fisher, *Phys. Rev.* **B40**, 546 (1989).
- [2] L. Amico and V. Penna, *Phys. Rev. Lett.* **80**, 2189 (1998).
- [3] Franco Dalfovo, Stefano Giorgini, Lev P. Pitaevskii, Sandro Stringari, *Rev. Mod. Phys.* **71**, 463 (1999).
- [4] T. Esslinger, I. Bloch, and T. W. Hänsch, *Phys. Rev.* **A58**, R2664 (1998)
- [5] S. Raghavan, A. Smerzi, S. Fantoni, and S. Shenoy *Phys. Rev.* **A59**, 620 (1999).
- [6] J. L. Martin, C. R. McKenzie, N. R. Thomas, and A. C. Wilson, cond-mat/9912045.
- [7] L. Guidoni, C. Trichè, P. Verkerk, and G. Grynberg *Phys. Rev. Lett.* **79**, 3363 (1997); K-P. Marzlin and W. Zhang, *Phys. Rev.* **A59**, 2982 (1999).
- [8] K. Berg-Sorensen and K. Molmer, *Phys. Rev.* **A58**, 1480 (1998).
- [9] W.M. Zhang, D.H. Feng, and R. Gilmore, *Rev. Mod. Phys.* **62**, 867 (1990).
- [10] A. Montorsi and V. Penna, *Phys. Rev.* **B55**, 8226 (1999).
- [11] A. Smerzi, S. Fantoni, S. Giovannazzi and S. Shenoy *Phys. Rev. Lett.* **79** , 4950 (1997).
- [12] H. T. Davis, *Introduction to Nonlinear Differential and Integral Equations*, (Dover, New York, 1970).
- [13] M. C. Gutzwiller, *Chaos in Classical and Quantum Mechanics*, (Springer-Verlag, New York, 1991).
- [14] L. D. Landau and E. M. Lifshits, *Quantum Mechanics*, (Pergamon, Oxford, 1957).
- [15] R. Burioni, D. Cassi, I. Meccoli, M. Rasetti, S. Regina, P. Sodano, A. Vezzi "Bose-Einstein condensation in inhomogeneous Josephson arrays", cond-mat/0004100
- [16] R. Franzosi and V. Penna, cond-mat/0103460.